

AE4304P: Stochastic Aerospace Systems Proctical

by

Lorenzo Terenzi 4465156

Contents

Introduction	iii
1 Stability Analysis	1
1.1 State spaces	1
1.2 Feedback controller	2
2 Time Domain Simulation	5
2.1 Lateral acceleration.	5
2.2 Response to turbulence	5
3 Spectral analysis	9
3.1 Power Spectral Densities	9
4 Variance analysis	14
4.1 Calculation methods	14
4.2 Results and discussion	14
5 Conclusion	16

Introduction

In this assignment we have analysed the asymmetric responses of two aircraft models to lateral turbulence. The turbulence dynamics is captured through the Dryden model and presents the following characteristics

$$L_g = 150 \text{ m}, \quad \sigma_{v_g} = 1 \quad (1)$$

where L_g is the lateral scale of turbulence and σ_{v_g} the variance of the gusts velocities. The two aircraft models used are:

1. complete state space for asymmetric responses
2. reduced state space to approximate the Ducht Roll with both roll angle and rate assumed to be zero $\phi = 0$. This implies that $\beta = -\psi$, where β is the side-slip angle and ψ the heading angle.

In chapter 1 we defined the augmented states space of the two models, assessed their stability and designed an appropriate controller to stabilise them if needed. In chapter 2 the states spaces were simulated and the state of the lateral acceleration was added to the systems. All the time simulation of the states were plotted. In chapter 3 from the time data of the simulation we computed the PSDs of the states. The PSDs were calculated analytically, using the transfer function and experimentally using the time data. Also a filter was applied to the experimental PSD to make it smoother. A discussion on the calculations methods and results it is included. From the PDSs and time data we estimated the variances of the states of the two model in chapter 4. The variances were calculated in 3 ways: using the analytically PSD, using the experimental PSDs and obtaining it directly from the time data.

Stability Analysis

In this chapter we will present the state spaces formulation for the both the complete and the reduced model. We will proceed to design controllers to ensure that both the systems are stable.

1.1. State spaces

To simulate the systems and analyse their stability it's convenient to express them in state space form. We augmented each state space with the states that describe the turbulence and their dynamics.

1.1.1. Complete state space

This state space contains the linear equations of motions that govern asymmetric aircraft responses. The states relating to the aircraft are: the side-slip angle β , the roll angle ϕ , the normalised roll rate $pb/2V$ and the normalised yaw rate $rb/2V$. The inputs to the aircraft state space are the aileron deflection angle δ_a and the rudder deflection angle δ_r .

Following the lecture notes [], to simulate turbulence we introduced other 6 states that represent the accelerations and velocities of turbulent air: $(u_g, u_g^*, \alpha_g, \alpha_g^*, \beta_g, \beta_g^*)$. Where u_g is the longitudinal gust velocity and u_g^* its time derivative, $\alpha_g = w_g/V$, the angle of attack change due to the vertical gust velocity w_g and α_g^* its time derivative, $\beta_g = v_g/V$ is the side slip angle due to the lateral gust velocity v_g and β_g^* its time derivative. The turbulent states are generated via Gaussian noises w_1, w_2, w_3 which are added as inputs to the state space system. Therefore the augmented state space is

$$\begin{pmatrix} \dot{\beta} \\ \dot{\phi} \\ \frac{pb}{2V} \\ \frac{rb}{2V} \\ \dot{u}_g \\ \dot{u}_g^* \\ \dot{\alpha}_g \\ \dot{\alpha}_g^* \\ \dot{\beta}_g \\ \dot{\beta}_g^* \end{pmatrix} = \begin{pmatrix} y_\beta & y_\phi & y_p & y_r & 0 & 0 & 0 & 0 & y_{\beta_g} & 0 \\ 0 & 0 & 2\frac{V}{b} & 0 & 0 & 0 & 0 & 0 & 0 & 0 \\ l_\beta & 0 & l_p & l_r & l_{u_g} & 0 & l_{\alpha_g} & 0 & l_{\beta_g} & 0 \\ n_\beta & 0 & n_p & n_r & n_{u_g} & 0 & n_{\alpha_g} & 0 & n_{\beta_g} & 0 \\ 0 & 0 & 0 & 0 & 0 & 1 & 0 & 0 & 0 & 0 \\ 0 & 0 & 0 & 0 & -\left(\frac{V}{L_g}\right)^2 \frac{1}{\tau_1 \tau_2} & -\frac{\tau_1 + \tau_2}{\tau_1 \tau_2} \left(\frac{V}{L_g}\right) & 0 & 0 & 0 & 0 \\ 0 & 0 & 0 & 0 & 0 & 0 & 0 & 1 & 0 & 0 \\ 0 & 0 & 0 & 0 & 0 & 0 & -\left(\frac{V}{L_g}\right)^2 \frac{1}{\tau_4 \tau_5} & -\frac{\tau_4 + \tau_5}{\tau_4 \tau_5} \left(\frac{V}{L_g}\right) & 0 & 0 \\ 0 & 0 & 0 & 0 & 0 & 0 & 0 & 0 & 0 & 1 \\ 0 & 0 & 0 & 0 & 0 & 0 & 0 & 0 & -\left(\frac{V}{L_g}\right)^2 & -2\frac{V}{L_g} \end{pmatrix} \begin{pmatrix} \beta \\ \phi \\ \frac{pb}{2V} \\ \frac{rb}{2V} \\ \dot{u}_g \\ \dot{u}_g^* \\ \dot{\alpha}_g \\ \dot{\alpha}_g^* \\ \dot{\beta}_g \\ \dot{\beta}_g^* \end{pmatrix} + \begin{pmatrix} 0 & y_{\delta_r} & 0 & 0 & 0 & 0 \\ 0 & 0 & 0 & 0 & 0 & 0 \\ l_{\delta_a} & l_{\delta_r} & 0 & 0 & 0 & 0 \\ n_{\delta_a} & n_{\delta_r} & 0 & 0 & 0 & 0 \\ 0 & 0 & \frac{\tau_3}{\tau_1 \tau_2} \sqrt{\frac{V}{L_g} I_{\dot{u}_g}(0, B)} & 0 & 0 & 0 \\ 0 & 0 & \left(1 - \frac{\tau_3(\tau_1 + \tau_2)}{\tau_1 \tau_2}\right) \frac{1}{\tau_1 \tau_2} \sqrt{\left(\frac{V}{L_g}\right)^3 I_{\dot{u}_g}(0, B)} & 0 & 0 & 0 \\ 0 & 0 & 0 & \frac{\tau_6}{\tau_4 \tau_5} \sqrt{\frac{V}{L_g} I_{\alpha_g}(0, B)} & 0 & 0 \\ 0 & 0 & 0 & \left(1 - \frac{\tau_6(\tau_4 + \tau_5)}{\tau_4 \tau_5}\right) \frac{1}{\tau_4 \tau_5} \sqrt{\left(\frac{V}{L_g}\right)^3 I_{\alpha_g}(0, B)} & 0 & 0 \\ 0 & 0 & 0 & 0 & \sigma_{\beta_g} \sqrt{\frac{3V}{L_g}} & 0 \\ 0 & 0 & 0 & 0 & (1 - 2\sqrt{3})\sigma_{\beta_g} \sqrt{\left(\frac{V}{L_g}\right)^3} & 0 \end{pmatrix} \begin{pmatrix} \delta_a \\ \delta_r \\ w_1 \\ w_2 \\ w_3 \end{pmatrix}$$

We refrain here from defining all the variable mentioned in the state space; they can be found in chapter 8 of the lecture notes [].

1.1.2. Reduced state space

For the simplified model we assumed that the roll angle and roll $\phi = p = 0$. This implies that $\beta = -\psi$, where ψ is the heading angle. Since there is only one degree of freedom left, β , that describes the rotation of the aircraft around the vertical axis, we only need only the moment equilibrium equation of motion around the z axis

$$C_{n_\beta}\beta + C_{n_\beta}\frac{b}{V}\dot{\beta} + \frac{b}{2V}C_{n_p}p + \frac{2b^2\mu_b K_{XZ}}{V^2}\dot{p} + \frac{b}{2V}C_{n_r}r - \frac{2b^2K_Z^2}{V^2}\dot{r} = -C_{n_{\delta_a}}\delta_a - C_{n_{\delta_r}}\delta_r \quad (1.1)$$

which since $\beta = -\psi$ and $\phi = p = 0$ can be rewritten as

$$-C_{n_\beta}\psi + \frac{b}{2V}C_{n_\beta}\dot{\psi} - 2\mu_b K_Z^2 \left(\frac{b}{V}\right)^2 \ddot{\psi} = 0 \quad (1.2)$$

Setting $\dot{\psi} = r$ we obtain the following state space system

$$\begin{bmatrix} \dot{\psi} \\ \dot{r} \\ \ddot{\psi} \end{bmatrix} = \begin{bmatrix} 0 & \frac{2V}{b} \\ C_{n_\beta} & \frac{C_{n_r}b}{2Va} \end{bmatrix} \begin{bmatrix} \psi \\ r \\ \ddot{\psi} \end{bmatrix} \quad (1.3)$$

where $a = -2\mu_b \left(\frac{bK_Z}{V}\right)^2$. If we augment it in the same way as the complete state space we obtain As before the turbulent

$$\begin{pmatrix} \dot{\psi} \\ \dot{r} \\ \ddot{\psi} \\ \dot{\alpha}_g \\ \dot{\alpha}_g^* \\ \dot{\beta}_g \\ \dot{\beta}_g^* \end{pmatrix} = \begin{pmatrix} 0 & \frac{2V}{b} & 0 & 0 & 0 & 0 & 0 & 0 & 0 & 0 & 0 \\ \frac{C_{n_\beta}}{a} & \frac{C_{n_r}b}{2Va} & 0 & 0 & 0 & 0 & 1 & 0 & 0 & 0 & 0 \\ 0 & 0 & 0 & 0 & -\left(\frac{V}{L_g}\right)^2 \frac{1}{\tau_1 \tau_2} & -\frac{\tau_1 + \tau_2}{\tau_1 \tau_2} \left(\frac{V}{L_g}\right) & 0 & 0 & 0 & 0 & 0 \\ 0 & 0 & 0 & 0 & 0 & 0 & 0 & 1 & 0 & 0 & 0 \\ 0 & 0 & 0 & 0 & 0 & 0 & -\left(\frac{V}{L_g}\right)^2 \frac{1}{\tau_4 \tau_5} & -\frac{\tau_4 + \tau_5}{\tau_4 \tau_5} \left(\frac{V}{L_g}\right) & 0 & 0 & 0 \\ 0 & 0 & 0 & 0 & 0 & 0 & 0 & 0 & 0 & 1 & 0 \\ 0 & 0 & 0 & 0 & 0 & 0 & 0 & 0 & -\left(\frac{V}{L_g}\right)^2 & -2\frac{V}{L_g} & 0 \end{pmatrix} \begin{pmatrix} \psi \\ \frac{rb}{2V} \\ \hat{u}_g \\ \hat{u}_g^* \\ \alpha_g \\ \alpha_g^* \\ \beta_g \\ \beta_g^* \end{pmatrix} + \begin{pmatrix} 0 & 0 & 0 & 0 & 0 & 0 & 0 & 0 & 0 & 0 & 0 \\ n_{\delta_a} & n_{\delta_r} & 0 & 0 & 0 & 0 & 0 & 0 & 0 & 0 & 0 \\ 0 & 0 & \frac{\tau_3}{\tau_1 \tau_2} \sqrt{\frac{V}{L_g} I_{\hat{u}_g}(0, B)} & 0 & 0 & 0 & 0 & 0 & 0 & 0 & 0 \\ 0 & 0 & \left(1 - \frac{\tau_3(\tau_1 + \tau_2)}{\tau_1 \tau_2}\right) \frac{1}{\tau_1 \tau_2} \sqrt{\left(\frac{V}{L_g}\right)^3 I_{\hat{u}_g}(0, B)} & 0 & 0 & 0 & 0 & 0 & 0 & 0 & 0 \\ 0 & 0 & 0 & \frac{\tau_6}{\tau_4 \tau_5} \sqrt{\frac{V}{L_g} I_{\alpha_g}(0, B)} & 0 & 0 & 0 & 0 & 0 & 0 & 0 \\ 0 & 0 & 0 & \left(1 - \frac{\tau_6(\tau_4 + \tau_5)}{\tau_4 \tau_5}\right) \frac{1}{\tau_4 \tau_5} \sqrt{\left(\frac{V}{L_g}\right)^3 I_{\alpha_g}(0, B)} & 0 & 0 & 0 & 0 & 0 & 0 & 0 \\ 0 & 0 & 0 & 0 & \sigma_{\beta_g} \sqrt{\frac{3V}{L_g}} & 0 & 0 & 0 & 0 & 0 & 0 \\ 0 & 0 & 0 & 0 & (1 - 2\sqrt{3})\sigma_{\beta_g} \sqrt{\left(\frac{V}{L_g}\right)^3} & 0 & 0 & 0 & 0 & 0 & 0 \end{pmatrix} \begin{pmatrix} \delta_a \\ \delta_r \\ w_1 \\ w_3 \\ w_2 \end{pmatrix}$$

states α_g and u_g are not necessary, but we included them to make use of the pre-programmed state space in the file *cit2a.m* provided by the lecturer.

1.2. Feedback controller

Before performing the simulation it is necessary to assess the stability of the systems and augment it if necessary. To make the aircraft more stable we can design a roll-damper of the form

$$\delta_a = K_\phi \phi + K_p p \quad (1.4)$$

1.2.1. Complete state space

To assess the stability of the state space we have generated a pole-zero map of the eigenvalues of the aircraft states. The poles of the system can be visualised in Figure 1.1, we excluded the poles due the augmentation of the system.

It is clear that the eigenvalue due related to the spiral mode is not stable enough and we need to design the controller to move the pole. The dutch-roll eigenmode, associated with the complex conjugate pair of poles, is not very damped

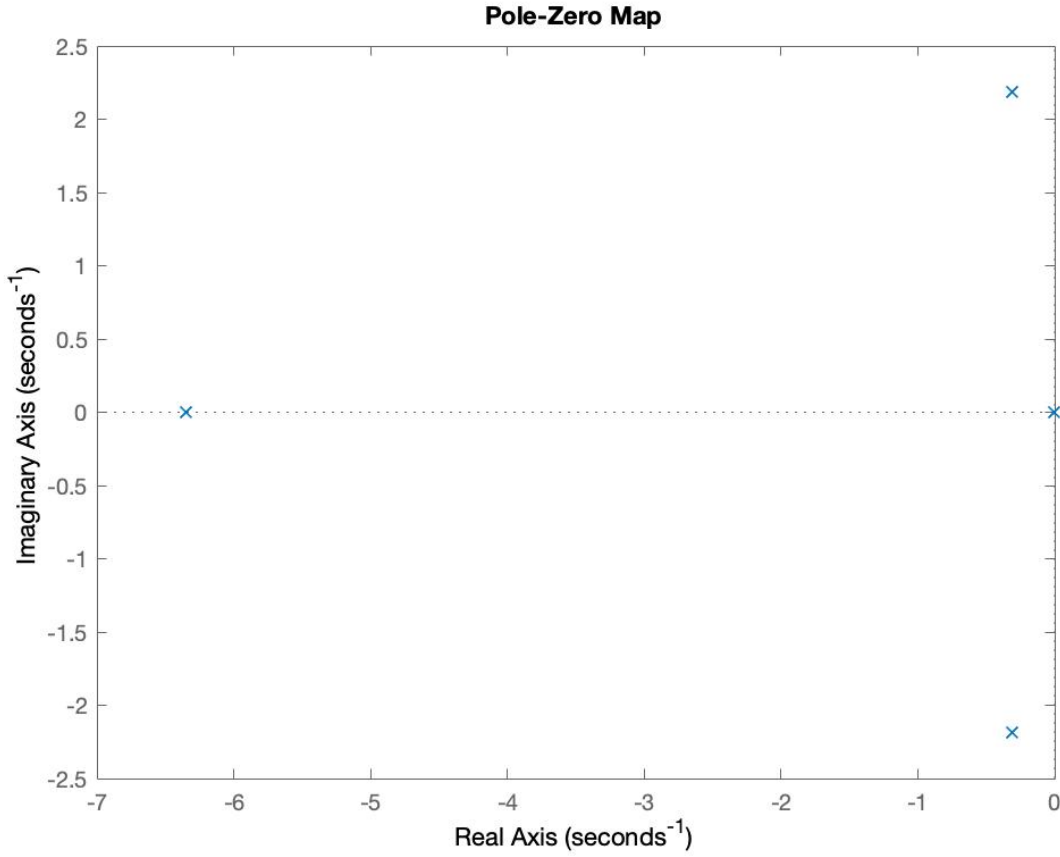


Figure 1.1: Pole-zero map of the aircraft

but given the shape of the controller the position of the poles can only be slightly changed. Finally the asymmetric roll eigenmode is damped fast enough. A more precise analysis of the poles characteristics can be seen in Table 1.1.

Since we want to modify only the spiral eigenmode we set $K_p = 0$ because the roll rate does play a big role in it, since the spiral is an inherently slow eigenmode. We chose the value of $K_\phi = -0.05$ to move the spiral pole at -0.35 , such that the time constant for the mode is $\tau = 2.83$ sec. The poles of the feedback system with $A_{new} = A - BK$, where $K = [0, K_\phi, 0, 0, \dots]$ can be seen in Table 1.2.

1.2.2. Reduced state space

The reduced state space poles, related to the Dutch roll, are located at $p_r = -0.288 \pm 2.19i$. Clearly since both ϕ and p are assumed to be equal to zero a roll-damper will not affect the location of the poles. We also notice that the Dutch roll motion is well represented by this model since the location of its poles is very close to the poles of the complete system.

Pole	Damping	Time Constant [sec]
-1.5×10^{-5}	1	6.62×10^4
$-0.308 + 2.19 i$	0.139	2.21
$-0.308 - 2.19 i$	0.139	2.21
-6.35	1	0.157

Table 1.1: Pole characteristics for the system

Pole	Damping	Time Constant [sec]
-0.35	1	2.83
$-0.313 + 2.20 i$	0.141	2.20
$-0.313 - 2.20 i$	0.141	2.20
-5.99	1	0.167

Table 1.2: Pole characteristics for the system with feedback

Time Domain Simulation

In this chapter we are going to show the how the aircraft respond to a lateral turbulence field with gust velocity $v_g = 1 \text{ ms}$ and turbulence scale $L_g = 1$.

2.1. Lateral acceleration

In this section we will simulate the state variable and the lateral accretion response for both the complete and reduced aircraft models. The lateral acceleration is given by

$$a_y \approx V(\dot{\beta} - \dot{\psi}) \quad (2.1)$$

where β is the side-slip angle and ψ the heading angle.

2.1.1. Complete state space

The lateral acceleration can be found directly from the state space. For the complete state space we need some simplification though to find a linear relation for ψ : the heading derivative can be expressed in the body frame as

$$\dot{\psi} = \frac{\sin \phi}{\cos \theta} q + \frac{\cos \phi}{\cos \theta} r \approx \phi q + r = r + O(q\phi) \quad (2.2)$$

We assumed the roll angle $\phi \ll 1$ and the pitch angle $\theta \ll 1$. Furthermore ignoring second order terms we find that $\dot{\psi} \approx r$. Now we find a_y from the state space augmenting the matrix C as follows

$$C_{aug} = [C; V(A(2,:) + [0, 0, 0, 2V/b, 0, \dots])] \quad (2.3)$$

2.1.2. Reduced state space

The lateral acceleration for the reduced state space system is equal to zero since $\beta = -\psi$

$$a_y = V * (\dot{\beta} + \dot{\psi}) = V * (\dot{\beta} - \dot{\beta}) = 0 \quad (2.4)$$

This is due to the fact that the aircraft is assumed to always have a roll angle equal $\phi = 0$.

2.2. Response to turbulence

The augmented state space has 5 inputs: 2 actuators and 3 Gaussian noise inputs. The white gaussian noise generated (following example 8.1 of the lecture notes) has an average power of $1/dt$

$$w = \frac{N(0, 1)}{\sqrt{dt}} \quad (2.5)$$

where $N(0, 1)$ is standard normal distribution and $1/dt$ is the sampling frequency. In Figure 2.1 can be seen the noise used to generate the response of the aircraft. The sampling time $dt = 0.05 \text{ sec}$ for a total simulation time of 60 seconds.

2.2.1. Complete state space

In Figure 2.2 can be seen the effect of lateral turbulence on the roll and side-slip angle while on Figure 2.5 its effects on the roll and yaw rate. Finally in Figure 2.6 the lateral acceleration due to turbulence is displayed. The maximum lateral acceleration reaches approximately 1 g.

2.2.2. Reduced state space system response

In this section we simulate the response of the reduced state showed in ???. In figure ?? both the heading ψ and its normalised derivative $rb/2V$ responses to turbulence are shown. In figure ?? we can observe that indeed the lateral acceleration for the simplified aircraft is equal to 0 at all times.

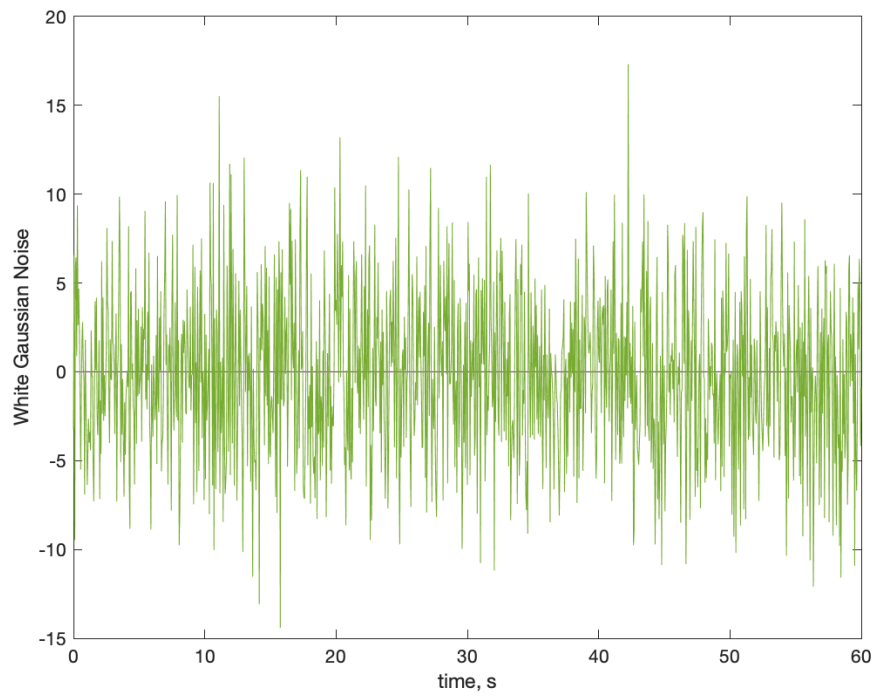


Figure 2.1: Gaussian white noise used for the simulation

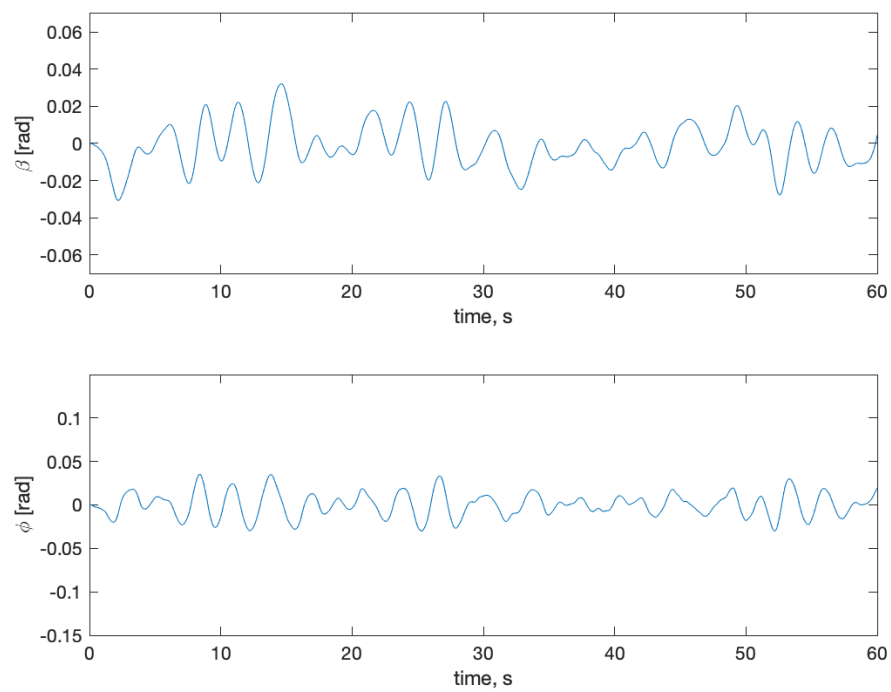


Figure 2.2: Roll angle and side-slip angle response to lateral turbulence for the complete model

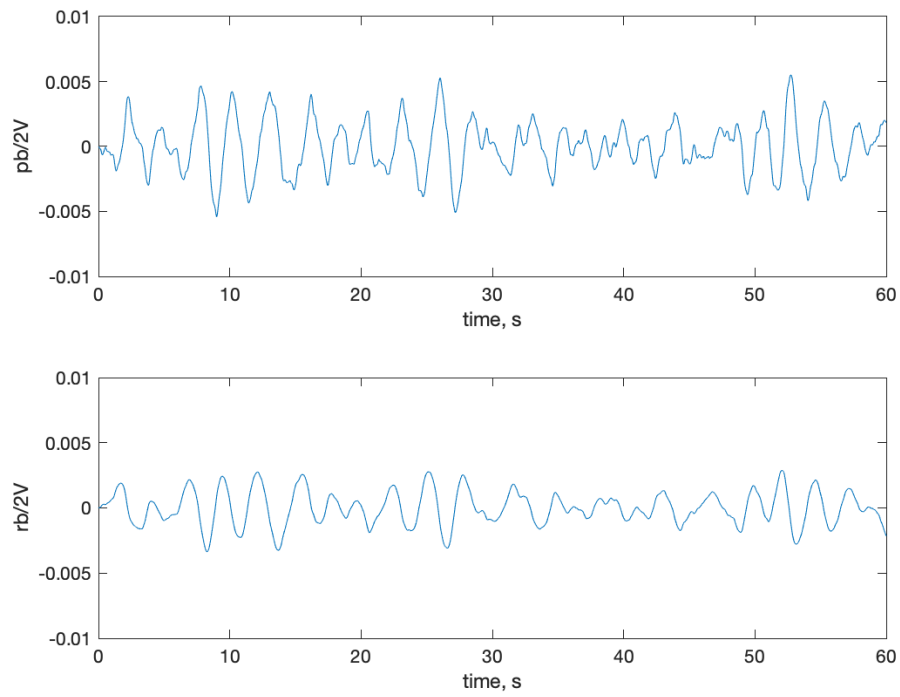


Figure 2.3: Roll and yaw rate responses to lateral turbulence for the complete model

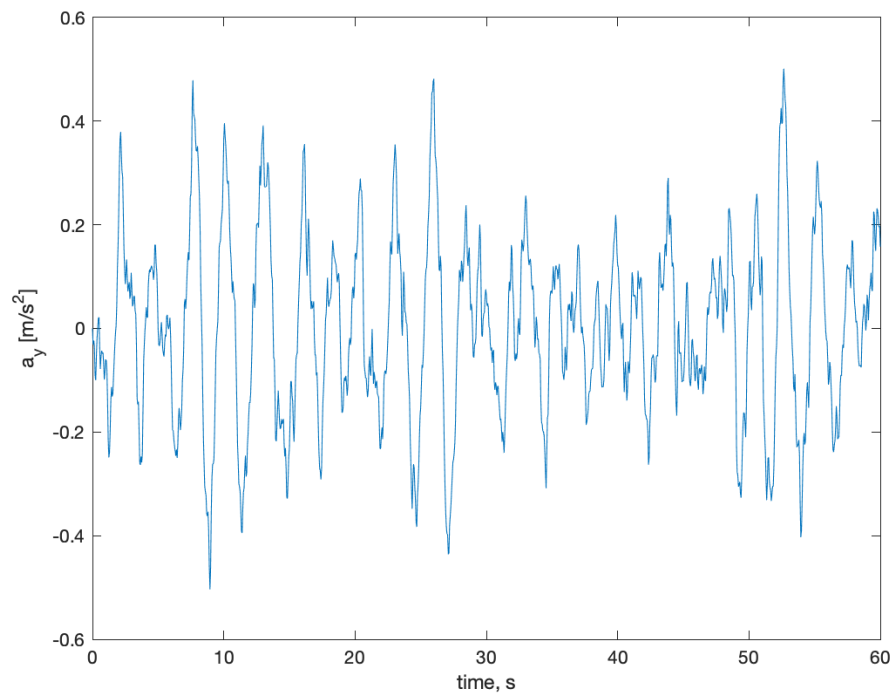


Figure 2.4: Lateral acceleration response to lateral turbulence for the complete model

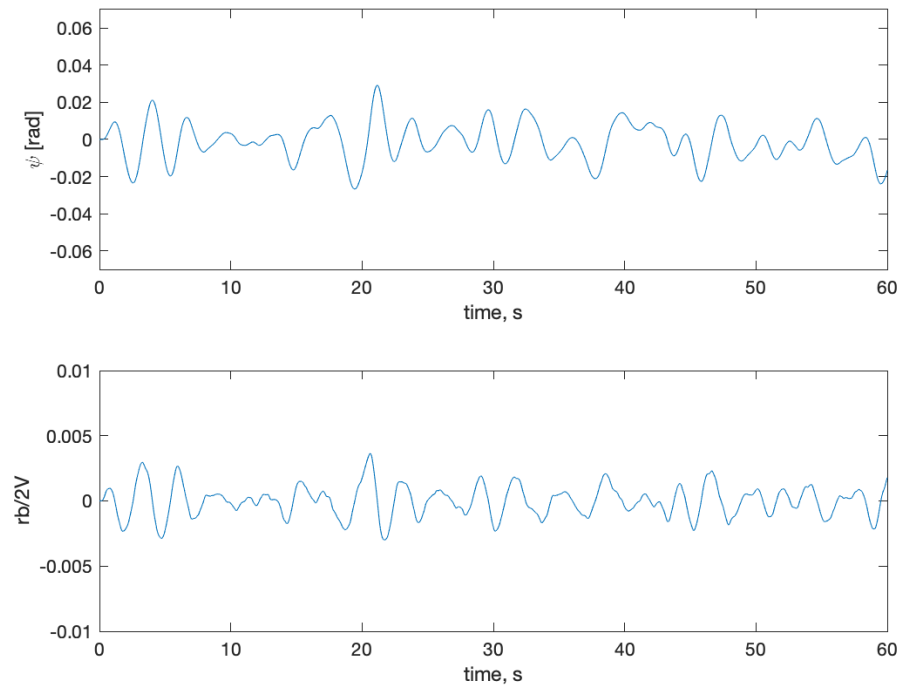


Figure 2.5: Heading and yaw rate responses to lateral turbulence for reduced model

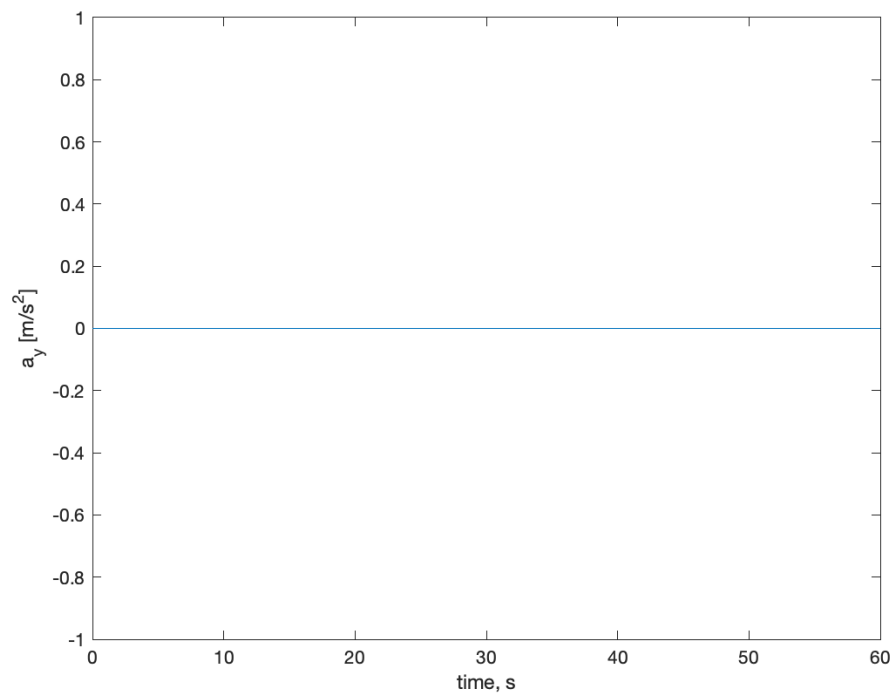


Figure 2.6: Lateral acceleration response to lateral turbulence for reduced model

Spectral analysis

In the chapter we calculated the power spectral densities of the states of the two aircraft models. For each state we found three power spectral densities: the analytical one, the experimental one and the experimental one with an applied filter.

3.1. Power Spectral Densities

The analytical power spectral densities of the states can be found by

$$S(\omega) = \|x(\omega)\|^2 \quad (3.1)$$

where the values of $X(\omega)$ can be found exactly since the transfer function of the system is known. In Matlab this can be easily done using the command *bode*. The experimental power spectral density can be found by fast Fourier transforming the time simulation data to obtain $X(k)$. The experimental power spectral density (PSD), which is an estimate of the true PSD, is given by

$$I_N(k) = \frac{dt}{N} \|x(k)\|^2 \quad (3.2)$$

where N is the number of samples and dt the sampling period. We can transform the index k , for $k < N/2$ into the corresponding frequency as follows

$$\omega = \frac{2\pi}{Ndt} k \quad (3.3)$$

Finally the filter that is applied on the periodogram I_N is

$$I_N(k) = 0.25I_N(k-1) + 0.5I_N(k) + 0.25I_N(k+1) \quad (3.4)$$

3.1.1. Complete state space

For the complete state space the pds of β, ϕ, p, r and a_y were generated. In Figure 3.1 are visible the pds of the sideslip angle β and roll angle ϕ . In Figure 3.2 are visible the PSD of the roll rate $pb/2V$ and the yaw rate $rb/2V$, finally in Figure 3.3 is shown the PSD of the lateral acceleration. In all the figures it is possible to see the analytical power spectral density, the experimental and the filtered experimental PSD.

3.1.2. Reduced state space

For the reduced state space the periodogram for the lateral acceleration was not generated since its time response is 0 for all times. Therefore only the PSD for the heading angle ψ and the roll rate $rb/2V$ were generated and they are visible in Figure 3.4. In the figures it is possible to see the analytical power spectral density, the experimental and the filtered experimental PSD.

3.1.3. Comparison of PSD for different methods

Let us analyse first the range and resolution of the found PSD. The analytical PSD has potentially infinite resolution and it is available for all frequencies if one has an analytical expression for the transfer function governing the system. On the other hand the experimental PSD has finite resolution and range. The resolution is related to the observation time T_{obs} : the minimum frequency resolution $\omega_0 = \frac{2\pi}{T} = \frac{2\pi}{Ndt} = 0.10$ rad/s. This can be observed directly on any plot of the experimental PSD since the first frequency plotted is indeed 10^{-1} , furthermore the plot results coarse at low frequencies. The range of the experimental PSD instead is limited by the sample frequency $\omega_s = \frac{2\pi}{dt} = 125.6$ rad/s. The maximum frequency detectable without aliasing is $\omega_{max} = \frac{\omega_s}{2}$, which is the maximum frequency plotted. The filtered PSD appears to be smoother than the experimental PSD based on a single realisation. Indeed in the plots are visible less oscillation and it appears on to track better the analytical PSD.

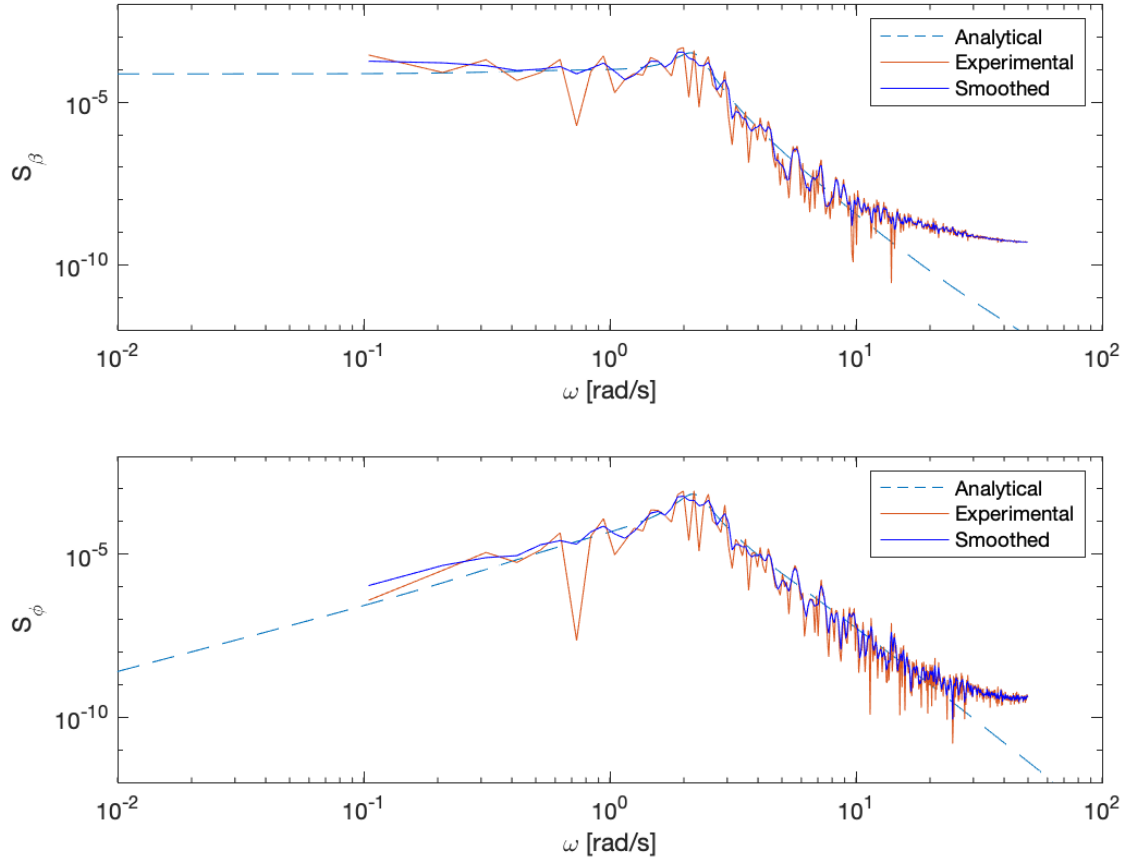


Figure 3.1: PSD of the states β and ϕ of the complete state space model

3.1.4. Comparison of the different models

The biggest difference is obviously the fact that we could not produce a meaningful PDS for the lateral acceleration for the reduced model. For the complete model its PSD for a_y shows that the most of the energy of the response is contained in the frequencies close to 1-2 rad/s. PSDs of ψ (reduced model) and β (complete model) are very similar to each other: they show the same shape and asymptotes of the analytical PSDs and the experimental one do not show significant deviation from each other. The same hold for the PDSs of the yaw rate for the complete and reduced model.

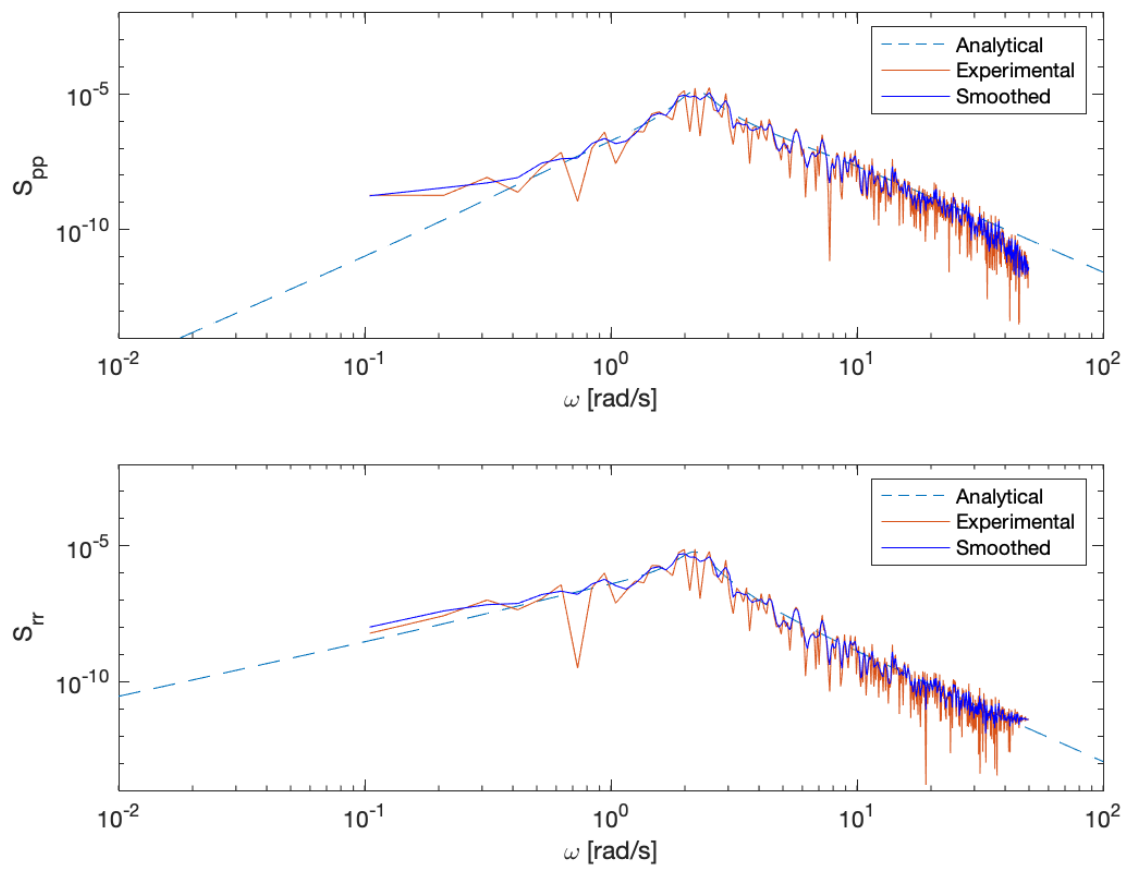


Figure 3.2: PSD of the states $pb/2V$ and $rb/2V$ of the complete state space model

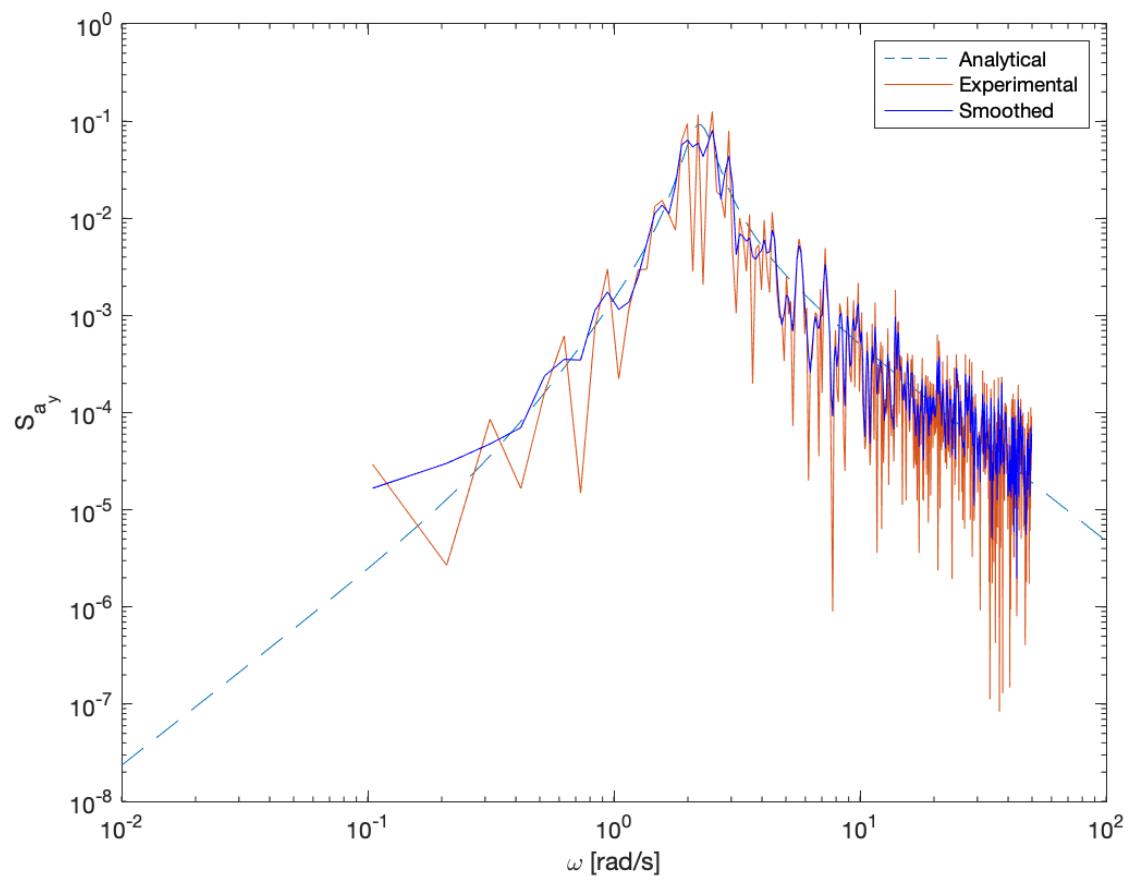


Figure 3.3: PSD of the lateral acceleration a_y of the complete state space model

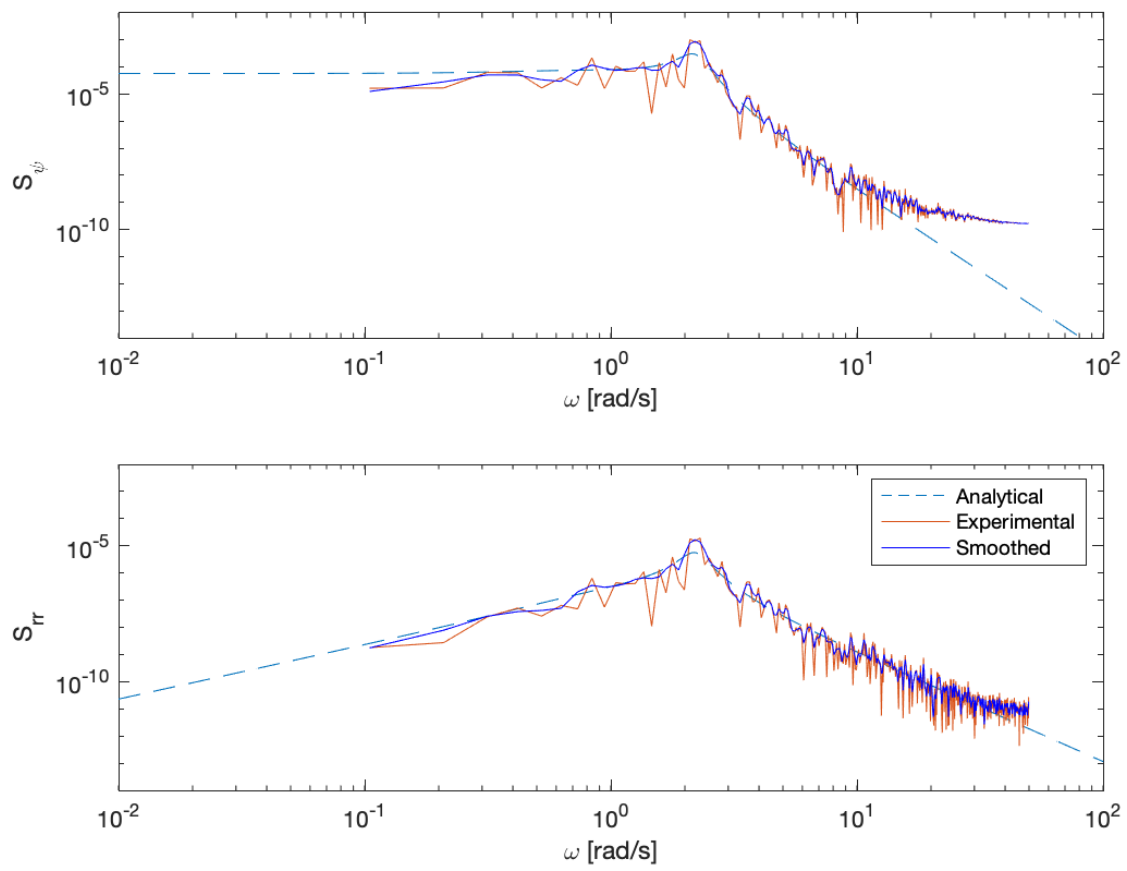


Figure 3.4: Pdf of the states ψ and $r b/2V$ of the reduced state space model

Variance analysis

In this chapter we calculated the variance of all the aircraft models' states and lateral acceleration.

4.1. Calculation methods

We calculate the variances of the states in three ways:

1. from the analytical PSDs
2. from the experimental PSDs
3. from the states' time data

The variance of the states is related to the PSDs by

$$\sigma_x^2 = \frac{1}{\pi} \int_0^\infty S_{xx}(\omega) d\omega \quad (4.1)$$

therefore the variance is calculated by numerically integrating via the trapezoidal method the analytical PSDs as

$$\sigma_x^2 = \frac{1}{\pi} \int_0^\infty S_{xx}(\omega) d\omega \approx \sum_{i=0}^M \frac{S_{xx}(i+1) + S_{xx}(i)}{2} \omega_{i+1} - \omega_i \quad (4.2)$$

similarly for the experimental PSD

$$\sigma_{x^2} \approx \sum_{i=0}^{N/2} \frac{S_{xx}(i+1) + S_{xx}(i)}{2} \omega_{i+1} - \omega_i \quad (4.3)$$

The variance from the data is calculated directly from its definition

$$\sigma_x^2 = \prod_{i=0}^N \frac{(x(t_i) - \mu)^2}{N} \quad (4.4)$$

where μ is the estimated mean of the data. Additionally the variance was calculated from an ensemble of 100 series of time data.

4.2. Results and discussion

In Table 4.1 are shown the calculated variances for the complete state space model while in Table 4.2 are shown the ones related to the reduced model.

State	Analytical Var	Experimental Var	Smoothed Var	Var from time data	Ensemble Var from time data
β	1.31×10^{-4}	1.277×10^{-4}	1.278×10^{-4}	1.272×10^{-4}	1.275×10^{-4}
ϕ	1.909×10^{-4}	1.786×10^{-4}	1.786×10^{-4}	1.786×10^{-4}	1.859×10^{-4}
$pb/2V$	3.83×10^{-6}	3.592×10^{-6}	3.592×10^{-6}	3.592×10^{-6}	3.736×10^{-4}
$rb/2V$	1.667×10^{-6}	1.561×10^{-6}	1.561×10^{-6}	1.561×10^{-6}	1.628×10^{-4}
a_y	2.98×10^{-2}	2.78×10^{-2}	2.78×10^{-2}	2.78×10^{-2}	2.91×10^{-2}

Table 4.1: Various variances calculated for the complete state space model of the aircraft

To analyse the different results arising from the different methods let's focus on the variances of the complete state space model, shown in Table 4.1. The time data, experimental and experimental smoothed variances do not almost any difference in values between them. In principle the variance resulting from the time data and the experimental PSD

State	Analytical Var	Experimental Var	Smoothed Var	Var from time data	Ensemble Var from time data
ψ	1.094×10^{-4}	1.013×10^{-4}	1.012×10^{-4}	1.013×10^{-4}	1.027×10^{-4}
$rb/2V$	1.467×10^{-4}	1.322×10^{-4}	1.322×10^{-4}	1.322×10^{-4}	1.399×10^{-4}
a_y	0	0	0	0	0

Table 4.2: Various variances calculated for the reduced state space model of the aircraft

should be the same: the underlying data set is the same and fast Fourier transforming the data results only in minor information losses due to the limited resolution and frequency range. Any difference is probably due to numerical integration errors.

The smoothing, or weighted averaging over a short window, of the PSD does not affect its integral and therefore the variances calculated over the experimental PSD and the smoothed version are practically the same.

On the other hand, the analytical variance appear to be higher slightly higher than the experimental one, this is could due to higher range of frequencies over which we are integrating or just inaccuracies due to the finite resolution and the random nature of the data. Increasing the observation period and sampling frequency, we observed that the trend remain (even though it lessens) but changing the seed for the random number generator we obtain sometimes the opposite effect, i.e the variance from the experimental PSD is higher than the analytical one. We conclude therefore that the difference between the variance calculated from analytical and experimental PSD, given a similiar range of frequencies, is to be ascribed to randomness of data and finite observation time.

Now that the difference between the calculation methods has been addressed we can focus on the difference that are present between the two aircraft models. The variance of the state variable ψ (for reduced model $\psi = -\beta$) is lower than the one of β and the same old for the yaw rate of the reduced model compared to the one of the complete model. The variances of the complete model were expected to be higher since the roll is coupled with the yaw and any change in the one will affect the latter. This results in a more complex and varying behaviour that is reflected in a higher variance.

Conclusion

In this assignment we have analysed the asymmetric responses of two aircraft models to lateral turbulence. The turbulence dynamics is captured through the Dryden model and presents the following characteristics

$$L_g = 150 \text{ m}, \quad \sigma_{v_g} = 1 \quad (5.1)$$

where L_g is the lateral scale of turbulence and σ_{v_g} the variance of the gusts velocities. The two aircraft models used are:

1. complete state space for asymmetric responses
2. reduced state space to approximate the Dutch Roll with both roll angle and rate assumed to be zero $\phi = 0$. This implies that $\beta = -\psi$, where β is the side-slip angle and ψ the heading angle.

We proceeded in chapter 1 in augmenting the system with the gusts states. The resulting complete and reduced state spaces are driven by white Gaussian noise. The reduced state spaces has only two states ψ and $rb/2V$. The complete states space had a pole at -1.5×10^{-5} resulting in a poorly damped spiral mode. To move the pole to -0.35 a feedback controller with $\delta_a = -0.05 \phi$ was designed. The reduced state space was already stable.

In chapter 2 we simulated all the aircraft states of the two model under lateral turbulence driven by white Gaussian noise. The total observation time was $T =$ and the sampling period was $dt =$. Furthermore the lateral acceleration state $a_y = V(\dot{\psi} + \dot{\beta})$ was introduced for both models. The complete model exhibited lateral accelerations up to approximately 0.5 m/s while the reduced model experienced a lateral acceleration equal to 0 at all times. As expected the states that were majorly affected by the lateral turbulence were β and $rb/2V$, since lateral gusts directly hit the rudder.

In ?? we calculated the PSDs for all the states of both models. The PSDs were calculated analytically, evaluating the transfer function at several frequencies and experimentally Fourier transforming the time data. A filter was applied to the experimental PSD to make it smoother. The different PSDs have generally the same trend and similar values, major deviation are found a very low and very high frequencies. The two model present very similiar PSD for β and $rb/2V$, as was to be expected since lateral turbulence mainly affects those two states.

In chapter 4 we found the variances associated to the states responses under lateral turbulence of the models. The variances were calculated in 3 ways: using the analytically PSD, using the experimental PSDs and obtaining it directly from the time data. The variance from experimental non smoothed and smoothed PSDs and from the time data were the same up to numerical integration error. Discrepancies were found with the variances calculated from the analytical PSDs which can be attributed to the inherent randomness (just one 1 realisation used) and finite observation time used to generate the experimental PSDs. The reduced model has slightly less variance in the state responses because there is no coupling between the rolling motion and the yawing motion that can perturb each other if one of two is excited under turbulence.

From the assignement we can conclude that lateral turbulence mainly affect the side-slip and the yawing rate of the aircraft. Furthermore the reduced state model with only β and $rb/2V$ is good enough to capture the behaviour of the whole aircraft under lateral turbulence.